LCLS-II Technical Note

Alignment requirement for the SRF cavities of the LCLS-II injector

LCLS-II TN-14-16

12/16/2014

R. K. Li, C. Papadopoulos, T. O. Raubenheimer, J. F. Schmerge, and F. Zhou

This Note describes the alignment tolerance of the SRF cavities in the LCLS-II injector.

When electron beams travel through a TM010 cavity with transverse position or angular offsets, the time-dependent transverse RF forces may cause emittance growth. This effect is particularly severe in the first SRF cavity following the electron gun, when the beam energy is low and the bunch length is long.

In this Note, we evaluate the emittance degradation due to the transverse position and angular offsets of the first SRF cavity. We study the case of Layout 2 [1]. The main components and their locations (in the unit of meter) in Layout 2 is shown in Fig. 1(bottom). It includes the VHF gun, Solenoid 1, the buncher, Solenoid 2, the first SRF cavity (Cav 1, or the capture cavity), a drift distance, and the standard cyromodule consisting of eight SRF cavities (Cav 2 – Cav 9). The distance between Cav 1 and Cav 2 centers is 5.47 m. The beam dynamics in Layout 2 is actually very similar to that of Layout 1, if in Layout 1 the 2nd to 4th cavities are turned off. It is reasonable to expect the alignment requirement to be similar for both Layouts.

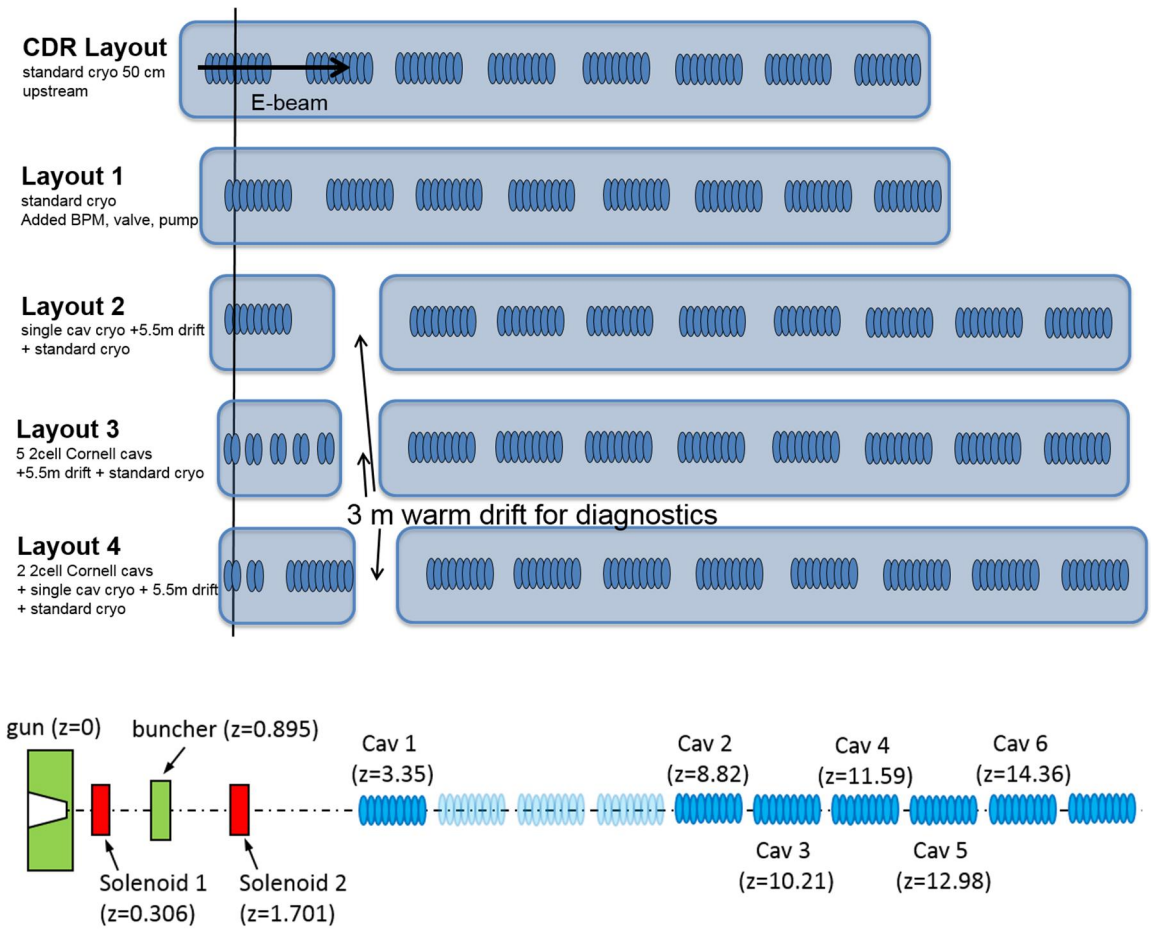

Figure 1. (Top) Various layouts of the LCLS-II injector (Adapted from [1]). (Bottom) A more detailed schematic of Layout 2. The cathode is located at z=0. The center positions of other elements are labelled. In Layout 1 the drift distance after Cav 1 is filled with three 9-cell cavities.

Some key beam and machine parameters are summarized in Table 1.

Table 1. Electron beam and machine parameters in Layout 2 of the LCLS-II injector.

Parameters	Values	Units
UV laser spot size, rms (uniform)	0.192	mm
Thermal emittance	0.192	mm-mrad
UV pulse length, FWHM (plateau)	33	ps
UV pulse rising edge	2	ps
Beam charge	100	pC
Gun frequency	187	MHz
Gun gradient	21.3	MV/m
Beam energy at gun exit	798	keV
Cav 1 gradient	15.6	MV/m

GPT is used for the results shown in this Note.

First, we reproduce in GPT the optimized results from ASTRA [2]. The initial beam distribution, filed maps, and the input file are translated from ASTRA to GPT. Besides the parameters included in the input deck, the cavity phases for maximum energy gain by ASTRA's auto-phasing function are required as the input in GPT. We noticed that the phase of the buncher and the strength of Solenoid 2 need to be adjusted in GPT to reach the optimal emittance obtained by ASTRA. The small discrepancy seem to be related to how image-charge forces and longitudinal space charge forces are modelled. The optimized GPT results is shown in Fig. 2.

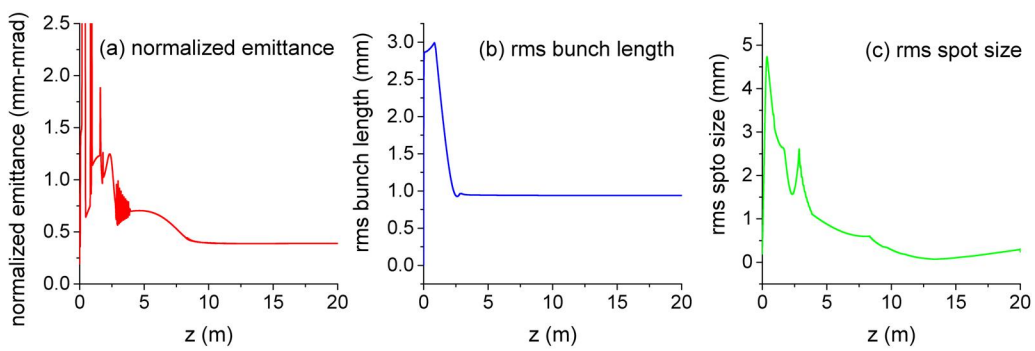

Figure 2. GPT simulation results of Layout 2:(a) normalized emittance, (b) rms bunch length, and (c) rms spot size.

To model the effects of the alignment error of Cav 1, we scan the horizontal position offset Δx and angular offset $\Delta x'$ of the Cav 1 field map (1-D map) and monitor the normalized emittance ε_n in both x and y planes at z=20 m. The change of x-emittance is shown in Fig. 3 while the y-emittance stays essentially constant. The injector is nearly axially symmetric and the simulation uses axially symmetric field maps with no vertical misalignments so there is no transverse coupling between the planes and thus the vertical misalignments are identical to the horizontal. The exception is the asymmetry due to the RF couplers (HOMs and power coupler) but these effects will be smaller than the misalignments described here and

thus will be considered in future studies.

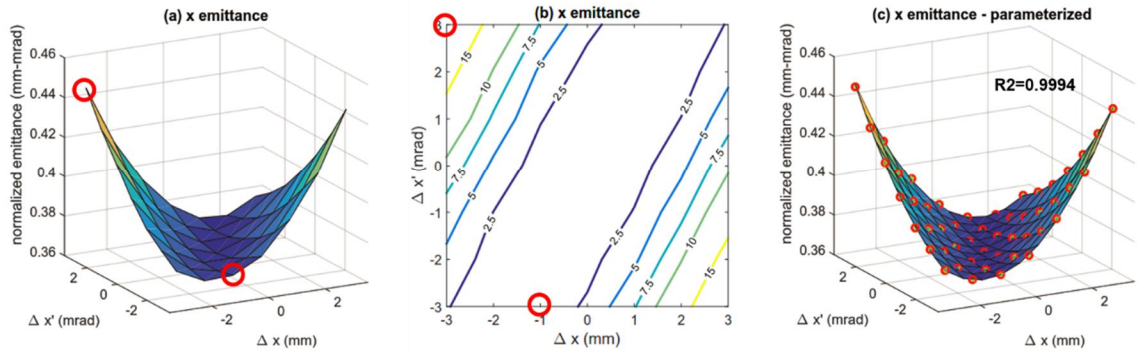

Figure 3. Normalized emittance in the x plane when Cav 1 is misaligned in horizontal position Δx and horizontal divergence Δx': (a) showing the absolute emittance numbers and (b) showing the percentage changes. (c)The GPT simulation results (red dot) are fitted with a 2nd-order polynomial function.

We re-plot Fig. 3(a) in Fig. 3(b) and express the emittance growth by percentage. To control the emittance degradation below 5%, the position offset should be less than 2 mm assuming no divergence error, or the angular offset less than 3.5 mrad assuming no position error.

It is possible to parameterize the GPT results as

$$\varepsilon_{nx} = 0.369 + 0.0037(\Delta x)^2 - 0.0038\Delta x\Delta x' + 0.0011(\Delta x')^2,$$

where the units for ε_{nx}, Δx, and $\Delta x'$ are mm-mrad, mm, and mrad, respectively. In Fig. 3(c) we show the GPT simulation results (red dots) and the fitted 2-D surface. We note that the coefficients in the above equation is for the particular optimized beam and machine settings and would be different for other cases. Assuming we can achieve a transverse position misalignment of 0.6 mm and a tilt misalignment of 0.5 mrad, as listed in the LCLS-II 1.3 GHz Cryomodule Physics Requirement Document [3], the misalignment induced emittance growth will be < 1%.

We noticed from Fig. 3 that under certain combinations of Δx and Δx', the emittance growth is very small. To better understand the partial cancelation between the Δx and Δx' induced emittance growth, we look into two cases, marked by the two red circles in Fig. 3: (i) Δx=-1 mm and Δx'=-3 mrad, and (ii) Δx=-3 mm and Δx'=3 mrad, and compare them with the ideal case (Δx=0 mm and Δx'=0 mrad). We plot in Fig. 4 (a) the beam center position in the x-direction 'avgx', (b) the average electric field in the x-direction 'avgfEx', (c) the normalized x-emittance 'nemixrms', and (d) zoomed-in plot of the x-emittance at Cav 1.

The much larger emittance growth in case (ii) is associated with the large transverse offset and strong transverse electric field at the low energy. Case (i) actually has larger offset and transverse electric fields at the downstream end of Cav 1 where the beam energy is high and the effect is small. Note the transverse electric field is time-dependent, thus will cause different slopes of the x-x' distribution of beam slices, leading to an increased project beam emittance.

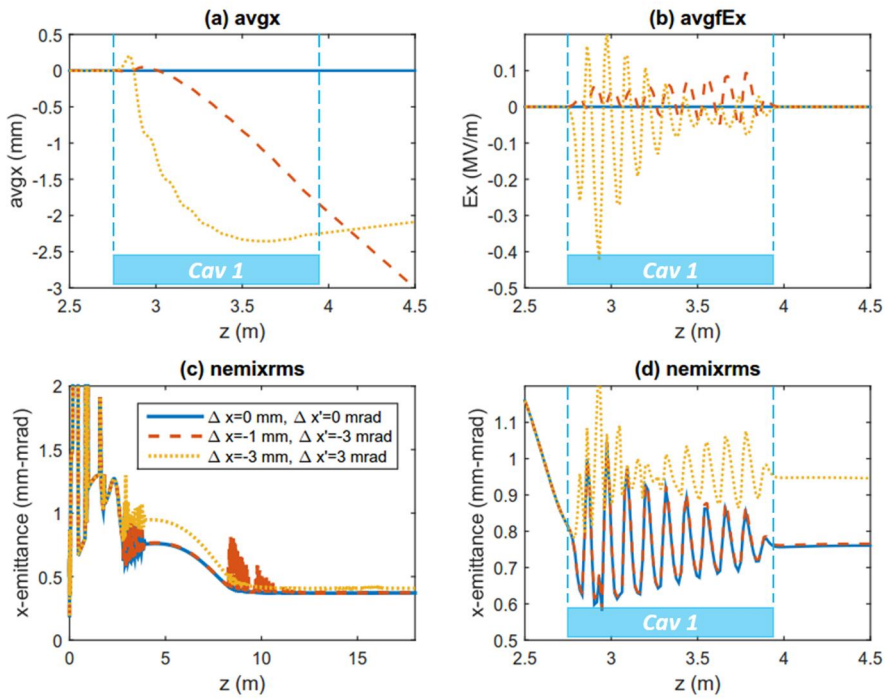

Figure 4. Comparison of (a) the beam center position, (b) transverse electric field, (c) x-emittance for (i) Δx=-1 mm and Δx'=-3 mrad, (ii) Δx=-3 mm and Δx'=3 mrad, and (iii) Δx=0 mm and Δx'=0 mrad. (d) is a zoomed-in plot of (c). The location and length of Cav 1 in indicated in (a), (b) and (d).

The same procedure can be used to analysis the alignment requirement for Cav 2, Cav 3, etc.

For a more in-depth understanding of misalignment induced emittance growth, we will study the dependence on beam energy, beam spot size, and bunch length in future studies.

References:

[1] J. F. Schmerge, presented at the DOE LCLS-II Status Review, Oct. 1st, 2014. (https://slacspace.slac.stanford.edu/sites/reviews/lclsii/LCLS-II_DOE_StatusRev2014/Presentations/Schmerge_Injector_DOER201409.pptx)

[2] Optimized ASTRA input files from F. Zhou and C. F. Papadopoulos.

[3] SCRF 1.3 GHz Cryomodule: LCLS-II Physics Requirements Document. (https://docs.slac.stanford.edu/sites/pub/Publications/SCRF_1.3_GHz_Cryomodule.pdf). The cavity to cyromodule X, Y misalignment is 0.5 mm, and the cyromodule to linac X, Y misalignment is 0.3 mm, thus the cavity to linac X, Y misalignment is $(0.5^2+0.3^2)^{1/2}$=0.6 mm. Similarly, the cavity tilt misalignment is 0.5 mrad.